RSC Advances

ROYAL SOCIETY OF CHEMISTRY

www.rsc.org/advances

Fabrication and Properties of Supramolecular Hybrid Hydrogel Doped with CdTe Quantum Dots

Xi Xie[1,2], Dong Ma[1,3] and Li-Ming Zhang[1]*

[1] PCFM Lab and GDHPPC Lab, Institute of Polymer Science, School of Chemistry and Chemical Engineering, Sun Yat-Sen (Zhongshan) University, Guangzhou, China

[2] Department of Materials Science and Engineering, Stanford University, Stanford, California, USA

[3] Key Laboratory of Biomaterials of Guangdong Higher Education Institutes, Department of Biomedical Engineering, Jinan University, Guangzhou 510632, China

*Correspondence and requests for materials should be addressed to Li-Ming Zhang, ceszhlm@mail.sysu.edu.cn.

Abstract

Fluorescent hydrogels incorporated with photoluminescent nanomaterials have achieved promising progress on bio-sensing or bio-labeling, yet the current techniques mostly rely on chemically cross-linked hydrogel which involved undesirable chemical reactions that may easily disturb the incorporated nanomaterials. In this work, the fabrication of fluorescent supramolecular hydrogel doped with semiconductor CdTe quantum dots (QDs) is demonstrated. The colloidal QDs were stabilized with synthetic amphiphilic block copolymer, mercaptan-ended poly(ethylene glycol)-poly(ε-caprolactone). The stability and fluorescent properties of the resultant colloidal QDs were evaluated. Fluorescent supramolecular hydrogel was fabricated based on the host-guest self-assembly between the amphiphilic block copolymer on the QD surface and added cyclic oligosaccharide host molecule, α-cyclodextrin (α-CD). The resultant photoluminescent hydrogel was characterized with rheology and X-ray diffraction, as well as photoluminescence spectra measurements. The gelation kinetics and mechanical strength of the supramolecular hydrogel can be modulated by

changing the amount of the used amphiphilic block copolymer, α-CD, or the incorporated QDs. These results suggest new opportunities for developing biocompatible optical materials with tunable fluorescent properties and mechanical properties.

Keywords: Quantum dots, Supramolecular hydrogel, Fluorescence, Amphiphilic block copolymer, cyclodextrin.

Introduction

With the development of nanotechnology, many nanomaterials including nanoparticles,[1–3] one-dimensional nanotubes[4,5] and nanowires[6,7] have attracted great research interest in the fields of electrical device, energy and biomedicine due to their unique nano-size, nanoscale features, and extraodinary properties.[8–11] In particular, fluorescent semiconductor nanoparticles, Quantum dots (QDs), have attracted extensive scientific and industrial interests as a consequence of their unique optical properties and electronic features, which give rise to many important applications in a variety of fields, including light-emitting devices,[12] photonic crystals,[13] biological labels and so on.[14–18] In contrast to organic fluorophores, QDs have many unique luminescence properties. For example, by controlling the particle size of QDs, their luminescence emission spectra (e.g. peak wavelength and distribution) can be precisely controlled.[19,20] QDs with different emission spectra can be excited by a broad range of wavelength, which is particularly useful when QDs with different luminescence emission need to be excited simultaneously.[21,22] In addition, the luminescence of QDs has high quantum yield and is resistant to photobleaching, which are significantly advantageous compared to conventional fluorophors.[17,18,23] Therefore, Significant progress has been made to explore QDs for electronic, energy, and biomedical applications.[12,17,23,24]

The dispersity and stability of QDs in aqueous solution is of significant importance on obtaining optical applications particularly in the field of biomedicine such as bio-labeling, bio-sensing and light-triggered drug delivery.[17,18,23] However,

due to a large surface-volume ratio and high free energy of the surface, QDs nanocrystals aggregate easily in aqueous medium leading to fluorescence quenching.[25,26] Therefore many surface functionalization techniques such as using ionic groups, synthetic polymer,[25] lipids[27] and proteins[28] have been employed to modify the surface of QD nanocrystals in order to stabilize the colloidal QDs.

On the other hand, hydrogels have attracted broad research interest due to their potential applications in biomedicine and tissue engineering as biocompatible delivery matrix for drugs, sensors or biological cells.[29–32] Particularly, fluorescent hydrogel that is responsive to chemical or thermal stimuli have been explored recently as optical sensors for PH, ions, glucose, or other biomolecular sensing.[33–39] Fabrication of fluorescent hydrogel by incorporating QDs in the polymer matrix has achieved promising success, as QDs provide robust and stable fluorescence emission and excellent sensitivity to stimuli after surface functionalization.[36,40] For example, Gatta´s-Asfura et al. successfully immobilized CdSe QDs within photo-curable poly(ethylene glycol) hydrogel.[41] Cao et al. modified CdTe QDs with cysteine in water, and waterborne polyurethane prepolymer nano-composite film incorporated with QDs was prepared.[42] In addition, Wu et al. developed boronic acid-based microgels that can reversibly detect glucose by immobilizing CdS QDs within microgel matrix.[34]

Up to mow, most of the reported QD-hydrogel systems are based on chemical gel, where the hydrogel were covalently cross-linked.[34,41,42] However, the preparation procedure of chemical gel normally involves chemical reactions, which may easily disturb the fluorescent property and surface properties of QDs. In addition, the sol-gel transition is generally irreversible after hydrogel formation, and there are concerns about the toxicity of chemical gel due to the release of un-reacted initiators or polymer monomers. These concerns limit the application of chemical gel especially in the biomedical fields. On the other hand, physical gels can be conveniently prepared with simple process and gentle experimental conditions, and the sol-gel transition is normally a reversible process.[43] Therefore fabrication of hybrid materials with physical hydrogel has attracted many research interests. In recent years,

supramolecular physical hydrogel, which is based on the host–guest interactions of cyclodextrins with synthetic polymers, has shown many promising applications in biotechnology including drug delivery, cell encapsulation, and bio-sensing.[44–48]

In this work, a novel route for the construction of fluorescent hydrogel doped with semiconductor QDs is demonstrated (Figure 1). Synthetic amphiphilic block copolymer, mercaptan-ended poly(ethylene glycol)- poly(ε-caprolactone) (PEG-PCL-SH), was used as the stabilizing agent for the preparation of colloidal CdTe QDs. In addition, this amphiphilic block copolymer served as the guest molecule for the inclusion complexation with cyclic oligosaccharide host molecule, α-cyclodextrin (α-CD).[44,45] As a result, hybrid supramolecular hydrogel with tunable gelation time, mechanical strength, and fluorescent property was fabricated based on the self-assembly between the amphiphilic block copolymer and α-cyclodextrin. In addition, the incorporation of fluorescent CdTe QDs with supramolecular-structured hydrogel provides a new strategy to modulate the physical and mechanical properties of the functional hydrogel nano-composites.

Materials and Methods

Reagents. Poly(ethylene glycol) monomethyl ether (MPEG, M_n = 5000) was purchased from Fluca and used after drying under vacuum at 80°C for 24 h. 3-mercaptocarboxylic acid (MPA) was purchased from Acros and used directly. ε-Caprolactone (ε-CL) was purchased from Sigma, which was dried by CaH_2 for 24 h and distilled prior to use. Stannous octoate (Sigma, USA) was used as received. α-Cyclodextrin (TCI, Japan) was used after drying under vacuum at 65 °C for 24 h. Cadmium chloride ($CdCl_2$) and tellurium (Te) powder were purchased from Acros and used directly. All other chemicals were analytical grade and used without further purification. The water used was Milli-Q ultrapure water.

Preparation and characterization of mercaptan-ended block copolymer PEG-PCL-SH.

Figure 2a shows the synthesis process of block copolymer PEG-PCL-SH, which includes two steps. In the first step, block copolymer PEG-PCL was prepared according to previously developed protocol.[45] Briefly, 1.5 g ε-CL (13 mmol) and 5.0 g

PEG (1.0 mmol) were added into a round bottom flask, and the mixture was heated with continuous stirring to produce a well-mixed molten phase under argon atmosphere. The mixture was then cooled, and stannous octoate (0.2 wt % of ε-CL) was added to the flask. The mixture was degassed and then heated to 120°. After stirring for 16 h, the mixture was cooled to room temperature. The product was dissolved in methylene chloride and then precipitated in ethyl ether. The block copolymer was filtered and dried overnight under vacuum, with a yield of 92% by weighting.

Block copolymer PEG-PCL was chain-end thiolated by esterification reaction with 3-mercaptocarboxylic acid using *p*-toluenesufonic acid as a catalyst.[47] Briefly, 10 mg *p*-toluenesufonic acid, 10 g PEG-PCL, and 1.38 g 3-mercaptocarboxylic acid were added into 100 ml toluene preheated to 120 ^{o}C. The reaction was allowed to proceed for 10 h under nitrogen atmosphere and driven forward by the continuous removal of water produced. The thiolated polymer was purified by precipitation in anhydrous ether, followed by using dichloromethane as solvent repeated for three times. The product was then dried under vacuum at room temperature for 24 h with a yield of over 80%.

The block copolymers were dissolved in CDCl$_3$ at room temperature and were characterized with Fourier Transform Infrared Spectroscopy (FTIR, Nicolet/Nexus 670) and MHz spectrometer (Mercury-Plus 300). Figure 2b shows the FTIR spectra of the polymers at different synthesis steps: PEG, PEG-PCL and PEG-PCL-SH. The absorption band at 1732 cm^{-1} (indicated with arrows) is corresponding to the stretch vibration absorption spectra of ester bonds on PCL units. Figure 2c shows the ^{1}H NMR spectrum of the block copolymer sample (PEG-PCL-SH). The peaks at 1.39, 1.65, 2.10, 2.31, and 4.06 ppm are assigned to the methylene protons of -(CH$_2$)$_3$-, -OCCH$_2$-, and -CH$_2$OOC- in PCL units, respectively. The sharp single peak at 3.64 ppm is attributed to the methylene protons of homosequences of the PEG oxyethylene units. The weak peak at 4.23 ppm is attributed to the methylene proton of the PEG end unit. The two small peaks at 2.76 and 2.95 ppm (indicated with a and b) were attributed to the methylene proton of 3-mercaptocarboxylic acid, which were different

from pure 3-mercaptocarboxylic acid. These analyses confirm the successful synthesis of the amphiphilic PCL-PEG-SH block copolymer. The number ratio of EG units and CL units in the block copolymer was determined by the ^{1}H NMR integral ratio to be 114:12, suggesting the formulation was EG_{114}-CL_{12}.

Preparation of aqueous colloidal CdTe QDs.

A series of aqueous colloidal CdTe QD solutions were prepared by adding freshly prepared NaHTe solution to N_2 saturated $CdCl_2$ solutions in the presence of the as-synthesized PEG-PCL-SH block copolymers as stabilizing agents.[49,50] Firstly, NaHTe were prepared by adding 80 mg sodium borohydride and 127.5 mg tellurium powder to a small flask, and then 1 mL of ultrapure water was added. The reaction system was cooled with ice bath. During the reaction, a small outlet connected to the flask was kept open to discharge the accumulated pressure from the resulting hydrogen. After approximately 8 h, the black tellurium powder disappeared and white precipitation of sodium tetraborate appeared on the bottom of the flask. The resulting NaHTe in clear supernatant was separated and used for the preparation of CdTe QDs.

In the next step, 12.0 mg $CdCl_2$ and a certain amount of PEG-PCL-SH polymer (Table 1) were dissolved in 20 mL ultrapure water, and 50 μL NaHTe solution was injected into the solution quickly under the N_2 atmosphere. The resulting mixture was distilled in room temperature for 10 minutes and then subjected to reflux. The reaction time was set to control the growth of the CdTe nanocrystals.

For the colloidal CdTe QDs encapsulated by PEG-PCL-SH, their size and morphology were characterized with transmission electron microscope (TEM, JEM-2100, JEOL, Japan). TEM samples were prepared by dropping colloid solution on copper grids and allowed to dry overnight at room temperature. Their colloidal stability in aqueous solution was evaluated with dynamic light scattering (DLS, Brooken Haven BI-200SM, U.S.A.). The samples were filtered with 0.45 μm-pore size filter, and then studied using DLS with a concentration of 3-5‰ and at 90° scattering angle. Photoluminescence (PL) spectra were recorded using a RF-5301PC spectrofluorimeter with a excitation wavelength of 375 nm.

Formation and characterization of supramolecular hydrogel.

A certain amount of aqueous α-CD solution (Table 2) was added into an aqueous solution of the colloidal QDs modified with PEG-PCL-SH. The mixture system was thoroughly stirred and set aside at ambient temperature overnight. Due to the supramolecular self-assembly between α-CD and the PEG, gelation occurred resulting in physical hydrogel network hybridized with CdTe QDs.

X-ray diffraction (XRD) measurements were performed with Rigaku D/max-2200 type X-ray diffractometer to characterize the hydrogel samples. Ni-filtered Cu Kα radiation with a wavelength of 0.154 nm was used as radiation source. The current was set to 40 mA and the voltage was set to 40 kV. Data was collected with the proportional counter detector at a rate of $2\theta = 1°$/min over the range of $2\theta = 5–70°$.

The gelation process was monitored using rheological method. The dynamic storage modulus (G') and loss modulus (G'') of the resultant hydrogel samples were measured at 25 °C by means of an advanced rheometric extended system (ARES, TA Co.). It was performed in oscillatory mode with a parallel plate geometry (50 mm diameter, 0.6 mm gap) and a frequency of 1 Hz. In order to prevent water from evaporating, a cover was coated around the geometry. To ensure the rheological measurements within a linear viscoelastic region, a dynamic strain sweep was conducted prior to the frequency sweep, and the corresponding strain was determined to be 1.0%. For the investigation of the hydrogel strength, the gelled system was allowed to age for 12 h at room temperature to complete gelation before the storage modulus of the resultant hydrogel sample was measured.

Photoluminescence (PL) spectra of hydrogels were recorded using RF-5301PC spectrofluorimeter with an excitation wavelength of 375 nm, same condition as measuring the fluorescence emission of the aqueous colloidal samples except a specific holder for solid gel samples was used. To investigate the dispersion of QDs within the gel, the samples were prepared with freezing microtomy and studied with TEM.

Results and Discussion

The stabilization of CdTe colloid in water is important for the fabrication of

supramolecular hydrogel. In this study, the CdTe QDs were encapsulated with amphiphilic PEG-PCL-SH block copolymer, which was designed to serve as effective stabilizing agent for colloidal QDs dispersion, as well as acting as the effective guest molecule for the supramolecular self-assembly with α-CD. Figure 3a shows a series of aqueous colloidal solution of CdTe QDs modified with PEG-PCL-SH at different preparation conditions. The optical properties of CdTe QDs can be affected by many factors, such as concentration of reagent, temperature of reaction, reaction time and so on. Figure 3b and 3c show the photoluminescence spectra of a series of colloidal CdTe QDs modified with PEG-PCL-SH at different polymer concentration and reaction time. The photoluminescence emission peak position of QDs shifts from 499 nm (cyanine emission) up to 549 nm (yellow emission) with reduction of the polymer concentration. The spectrum changing is mainly due to the changing of the CdTe QD size, where increased particle size leads to red shift of the spectrum.[20,49] The increased polymer concentration of polymer produces a thicker layer surrounding the CdTe nanocrystal surface, which inhibits the growth of the nanocrystals and hence leads to smaller particle size with shorter emission peak wavelength. On the other hand, the increased reaction time leads to larger particle size with longer fluorescent emission peak wavelength.

Figure 3d shows the typical TEM images of 2.5%-Sol QD colloid. The QDs dispersed well in water, which indicates the stabilization of CdTe nanocrystals with amphiphilic PEG-PCL-SH. The colloidal QDs solutions showed a macroscopically homogeneous dispersion for one month. Figure 3e and 3f show the particle size and fluorescence emission intensity as a function of time for a series of colloidal CdTe QDs modified with polymer of different concentration. The diameters of the colloidal QDs modified by polymers were approximately 20 nm based on DLS measurement, and they changed very little with increasing storage time up to two weeks. The 1.0%-Sol and 2.5%-Sol samples showed very little changing of their particle diameters after two weeks' storage. This result indicates that the PEG-PCL-SH copolymer acted as an effective agent that stabilizes the colloidal CdTe nanocrystals in water. Another sample with higher polymer concentration, 5.0%-Sol, appeared to

be less stable with time compared to the other two samples. This is likely because the PCL segments can degrade in the oxidation environment,[51] which can disturb the stability of the colloidal system. Since the 5.0%-Sol sample contains a higher amount of PCL, it is likely to be more sensitive to the PCL degradation and hence is less stable.

Gelation could occur at room temperature when the colloidal CdTe/PEG-PCL-SH dispersion was mixed with an aqueous solution of α-CD. This phenomenon was attributed to the inclusion complex formation between PEG-PCL-SH and α-CD, which results in the formation of supramolecular-structured hydrogel.[44,45,52] To confirm this, XRD measurements were conducted for pure α-CD, pure PEG-PCL-SH, hydrogel without QDs (native), and hydrogel with QDs (hybrid). As the XRD patterns shown in Figure 4a, the hydrogel samples had two characteristic diffraction peaks at $2\theta = 19.8$ (d = 4.44 Å) and 22.6° (d = 3.94 Å), which are assigned to the {210} and {300} reflections from the hexagonal lattice with $a = 13.6$ Å. The strong {210} reflection is a typical peak observed for polymer inclusion complexes with α-CD, which was obviously different from the peaks of pure α-CD and pure PEG-PCL-SH.[45,53] These results indicates that supramolecular-structured hydrogel formed by the inclusion between PEG-PCL-SH and α-CD. Because the amount of CdTe nanocrystals was much smaller compared to the polymer and α-CD, the XRD pattern of hybrid hydrogel did not show obvious typical peaks of QDs.

Due to the incorporated QDs, this supramolecular hydrogel can emit fluorescence under UV light excitation (Figure 4b). The TEM image of the hybrid hydrogel (Figure 4c) suggests that the CdTe QDs were still well-dispersed in the hydrogel matrix without obvious aggregation or agglomeration. The photoluminescence spectra of the hybrid hydrogel were measured with spectrofluorimeter as shown in Figure 4d. The CdTe QDs-doped hydrogel inherited the fluorescent properties of its corresponding colloidal solution (Supporting Information S4). As shown in Figure 4e, for samples with three different concentrations of polymer (1%, 2.5% and 5%), the hybrid hydrogels incorporated with QDs had similar photoluminescence emission peak position as their

corresponding colloidal solution (wavelength difference < 1%). The emission peak width of each sample was calculated by measuring the wavelength position at the semi-amplitude of the peak intensity. As shown in Figure 4f, the emission peak distributions of the hydrogel were slightly broader compared to the corresponding colloidal solution (increased by roughly 50%). This phenomenon of spectral broadening for the hybrid hydrogel is likely because the QDs have wider particle size distribution within the hydrogel matrix. As illustrated in Figure 4g, the QDs tend to have more uniform distribution in colloidal solution phase. While distributed in the hydrogel matrix, some QDs may aggregate which reduces the uniformity of the particle size, and hence leads to the broadening of the emission peak.

The strength of the hybrid fluorescent hydrogel was evaluated with advanced rheometric extended system. The hydrogel strength was determined by measuring the storage modulus (G') and loss modulus (G'') as a function of angular frequency. Figure 5a-c show the effects of the PEG-PCL-SH concentration, the α-CD amount, and the incorporation of the QDs on the hydrogel strength. It was found that the G' values for most samples were almost independent of the frequency for the investigated hydrogel samples. This confirms that the resultant supramolecular-structured hydrogel behaved as gel or "solid-like" fluid.[54] In addition, a significant increase in the storage modulus, G', was observed with the increase of PEG-PCL-SH concentration (Figure 5a) or α-CD amount (Figure 5b). When the CdTe nanocrystals were incorporated, the hydrogel strength increased obviously (Figure 5c). Based on the these results, schematic illustrations for the structure of the hybrid hydrogel were proposed in Figure 6a and 6b. The hydrophobic interactions between the PCL blocks facilitate the micellization of the PEG-PCL-SH with hydrophobic PCL as internal cores and hydrophilic PEG as the external shells. The inclusion complexes formed by α-CD and PEG-PCL-SH aggregate into microcrystals, which function as physical cross links and induce the formation of a supramolecular polymer network. In addition, the micellization of the PCL block may facilitate the formation of the polymer network. The inclusion complexation of α-CD with the PEG block together with the hydrophobic interaction between the PCL blocks results in the

gelation of the supramolecular hydrogel (Figure 6a).[55] For the hybrid hydrogel doped with QDs, the mercaptan-ended PCL blocks covalently attaches to the CdTe nanocrystals besides the hydrophobic interaction (Figure 6b).[56] This covalent interaction increases the strength of the cross links. Therefore the strength of the hybrid hydrogel is higher than the native hydrogel without QDs (Figure 6b). Based on these results and hypothesis, the strength of the hybrid hydrogel can be tuned by controlling the amount of the PEG-PCL-SH, α-CD, or the incorporated QDs.

The gelation kinetics were investigated with rheological monitoring to evaluate how the concentration of PEG-PCL-SH, α-CD amount, and the incorporated QDs affect the rate and extent of gelation. Time sweep measurement for the viscoelastic properties of the samples was conducted, in which the storage modulus (G') and loss modulus (G'') were monitored as a function of time upon the addition of α-CD. Gelation occurs when the storage modulus exceeds the loss modulus. The crossover point between G' and G'' implies the time point when sol–gel transition begins to occur. Beyond the crossing, the G' value exceeds the G'' value, indicating that the solution becomes more elastic.[57] The gelation time is defined to be the time interval between the addition of α-CD into the system and the formation of hydrogel, which is when $G' \geq G''$. Figure 7a-c show the time dependence of G' and G'' for three samples with different PEG-PCL-SH concentrations (1.0%, 2.5% and 5.0%). When the colloidal solution of QDs modified with 1.0% PEG-PCL-SH was mixed with 10% α-CD of equal volume, there is no distinguish evident that G' was higher than G'' values within 140 min after the addition of 10% α-CD, which suggests that the viscosity of the sample was low and no sol-gel transition occurred (Figure 7a). Extended incubation of the mixture solution for several hours yielded hydrogel eventually. In contrast, gelation can readily occur on the 2.5%-Gel (within 32.0 min) and 5.0%-Gel samples (within 15.4 min) as shown in Figure 7b and 7c. The gelation time decreases with the increase of the PEG-PCL-SH concentration. Similarly, the increase of α-CD amount from 5% to 15% encouraged gelation (Figure 7d-f). As shown in Figure 7f, sol-gel transition rapidly occurred within 2 min when 2.5%-Sol was mixed with 15% α-CD, while gelation took much longer time (88.3 min) when

the 2.5%-Sol was mixed with 5% α-CD (Figure 7d). These results suggest that the increase of PEG-PCL-SH or α-CD amounts is favorable for the formation of the supramolecular hydrogel. In addition, the incorporation of CdTe nanocrystals was found to facilitate gelation (Figure 8a and 8b). Compared with native hydrogel without QDs, the hybrid hydrogel doped with QDs has short gelation time and enhanced elasticity. This is likely because the covalent interaction of PEG-PCL-SH with the QDs is favorable for the subsequent inclusion complexation between PEG-PCL-SH and α-CD.[58]

Conclusion

In summary, a novel route for the construction of a fluorescent supramolecular hydrogel was developed in this work. Amphiphilic PEG-PCL-SH block copolymer was applied as an effective stabilizing agent for the preparation of colloidal CdTe QDs solution, and served as effective guest molecule for the supramolecular self-assembly in the presence of α-CD. The fluorescent properties and stability of the as-synthesized QD solution were systematically evaluated. The photoluminescence properties of the resultant QDs-doped hydrogel inherited from the polymer-modified QDs. The gelation kinetics and mechanical strength of the supramolecular hydrogels can be modulated by controlling the amount of PEG-PCL-SH, α-CD, or incorporation of CdTe QDs. This work offers a novel approach to fabricate fluorescent physical hydrogel based on supramolecular self-assembly. In addition, it should be noted that this hydrogel may contain some biology-favorable aspects such as biocompatibility, since, first, the amphiphilic polymer PEG-PCL-SH provides biocompatible encapsulation for the CdTe QDs that would effectively reduces the cytotoxicity of the QDs (Supporting Information Figure S5 and S6), and, second, the α-cyclodextrin that used for hydrogel self-assembly is a chemical that has been well used for medical, healthcare, food, and beverage applications, and has been approved for use by FDA. Therefore the hydrogel developed in this work is promising material for biomedicine-related applications. However, given that the present work is completely focusing on the fabrication and characterization of this novel fluorescent hydrogel material. A first step of the current work has been to grant successful fabrication of the

material, while the biology-related aspects of this fluorescent hydrogel would be definitely promising and attractive to explore in future work. Clever design of the incorporated quantum dots or polymers to be responsive to external stimuli such as PH, ions, biomolecules, chemicals or temperature allows these hydrogel as smart materials for a range of sensing or labeling applications. A first step of the current work has been to grant successful fabrication of the material. Truly responsive to external stimuli presents a new frontier and future steps to realize these supramolecular hydrogel as biocompatible optical materials or implantable optical sensors for bio-sensing or bio-labeling.

Table of Content
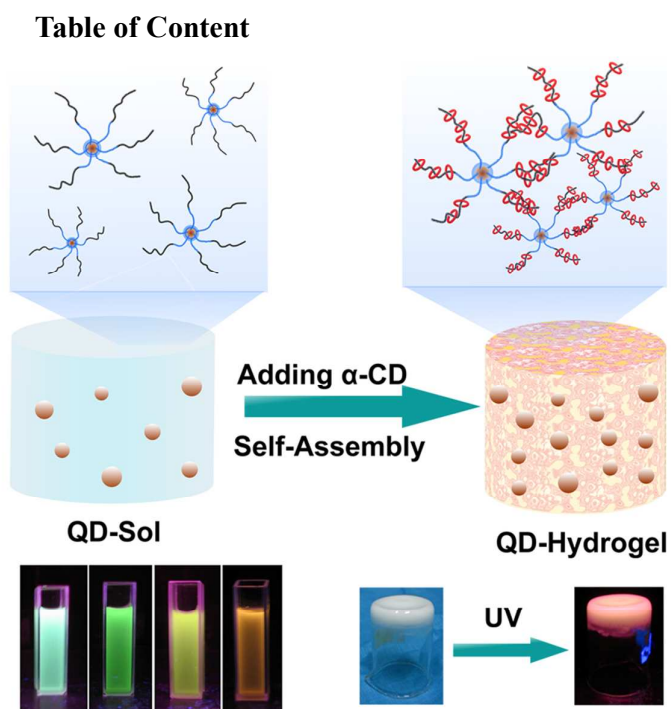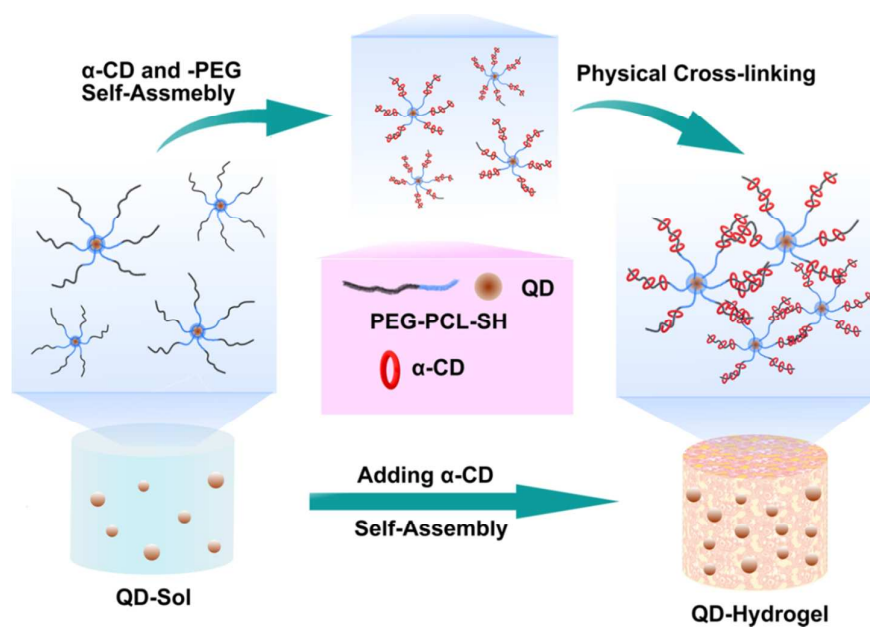
Figure 1. Schematics of the fabrication of fluorescent supramolecular hydrogel based on the host-guest self-assembly between α-CD and the amphiphilic block copolymer on the QD surface.
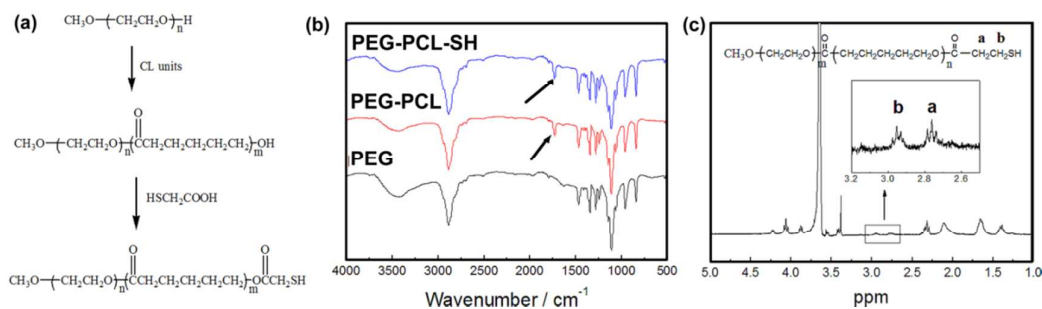

Figure 2. (a) Synthesis process of block copolymer PEG-PCL-SH. (b) The FTIR spectra of PEG, PEG-PCL and PEG-PCL-SH. (c) The ^{1}H NMR spectrum of the PEG-PCL-SH block copolymer in CDCl$_3$.

Table 1. The feed composition for the preparation of QD colloid solutions

Sample	PEG-PCL-SH / %	QDs [a] / mmol•L⁻¹	Reaction time / h
1.0%-Sol	1.0	3.0	1
2.5%-Sol	2.5	3.0	1
5.0%-Sol	5.0	3.0	1

[a] Calculated by the Cd element in the system.

Table 2. The feed composition for hydrogel preparation

Sample	PEG-PCL-SH / %	QDs / mmol•L⁻¹	α-CD / %
1.0%-Gel	0.5	1.5	5
2.5%-Gel	1.25	1.5	5
5.0%-Gel	2.5	1.5	5
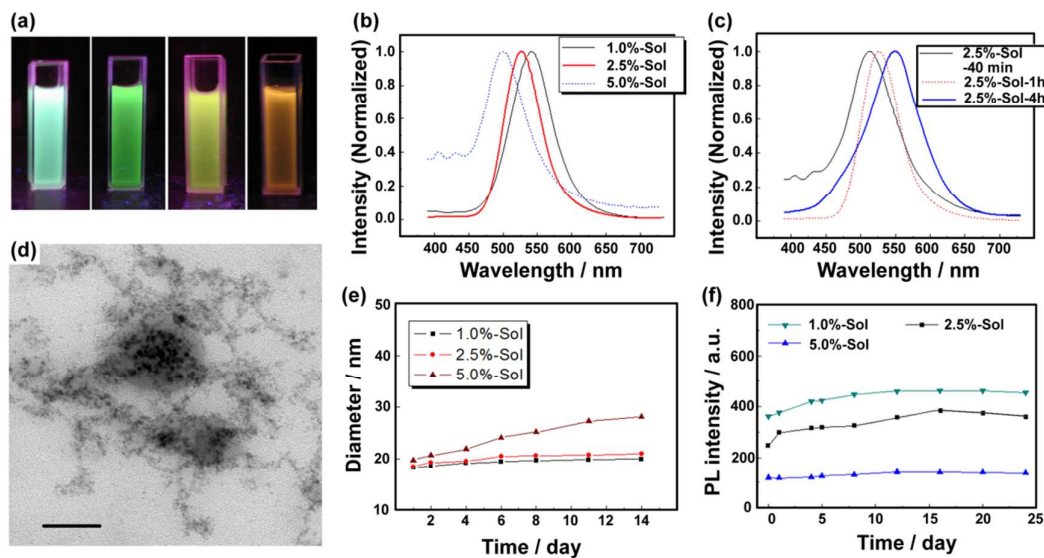
Figure 3. (a) Photography of a series of colloidal solution of CdTe QDs modified with PEG-PCL-SH. The fluorescence was excited with a UV lamp. (b) and (c) Photoluminescence spectra of a series of colloidal CdTe QDs modified with PEG-PCL-SH at different (b) polymer concentration and (c) reaction time. (d) TEM

images of 2.5%-Sol. Scale bar: 50 nm. (e) Particle sizes and (f) fluorescent intensities as a function of storage time.
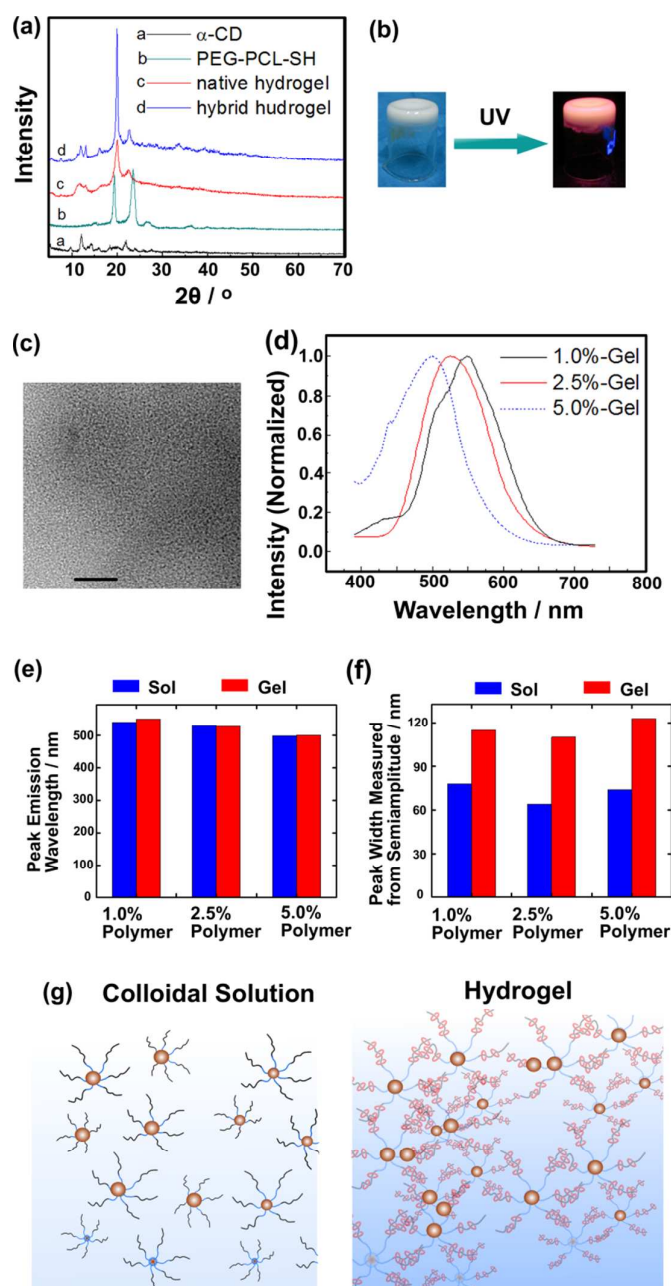

Figure 4. (a) X-ray diffraction patterns of PEG-PCL-SH, α-CD, native hydrogel sample, and hybrid hydrogel doped with QDs. (b) Photography of hydrogel doped with CdTe QDs. The fluorescence was excited with a UV lamp. (c) TEM images of 2.5%-Gel. Scale bar: 100 nm. (d) Photoluminescence spectra of a series of hydrogel doped with colloidal CdTe QDs. (e) Photoluminescence emission peak wavelength

and (f) peak width of a series of QD colloidal solution and hydrogel doped with QDs.

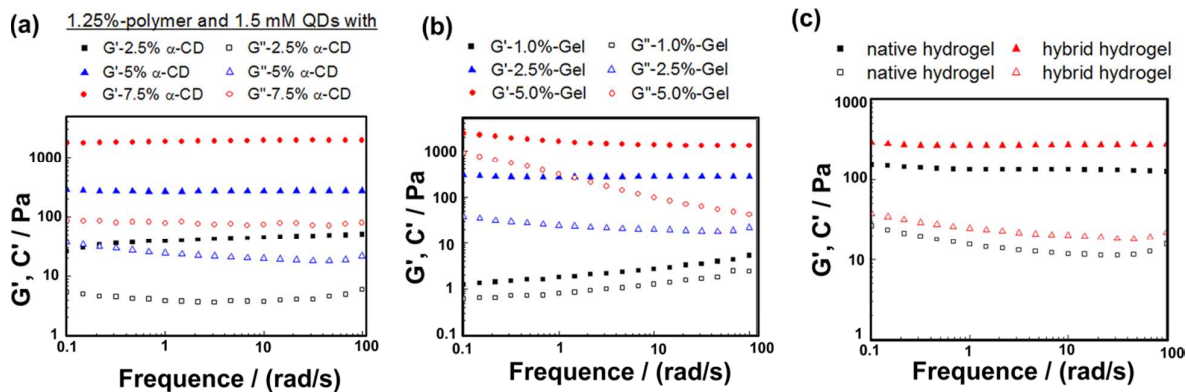(g) Schematics of QD distribution in colloidal solution and hydrogel.

Figure 5. Effects of (a) PEG-PCL-SH concentration, (b) α-CD amount, and (c) the incorporation of QDs on the hydrogel strength.
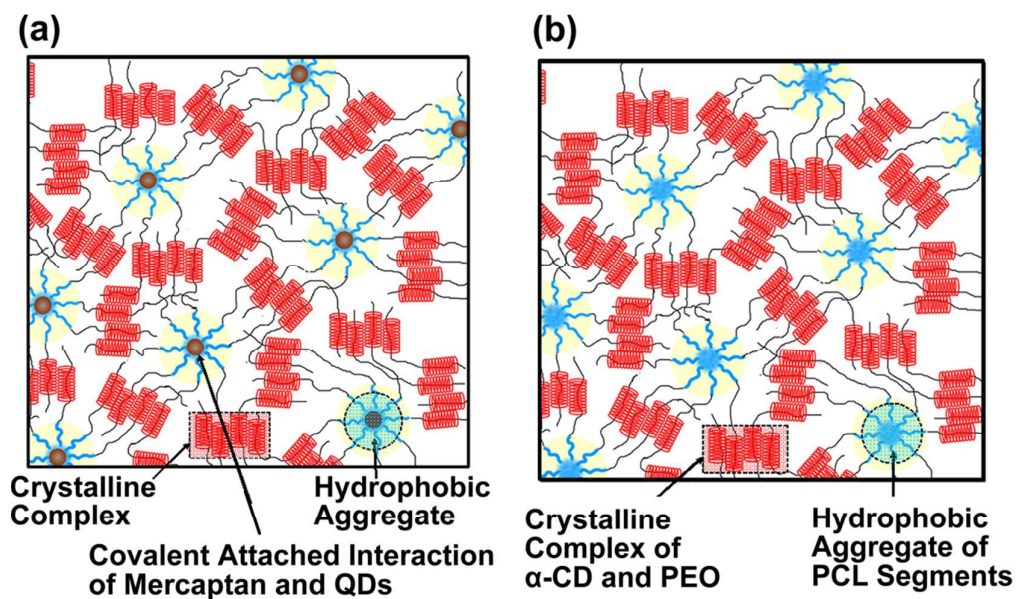

Figure 6. Schematic illustration of the structures of (a) native and (b) hybrid hydrogel doped with QDs.
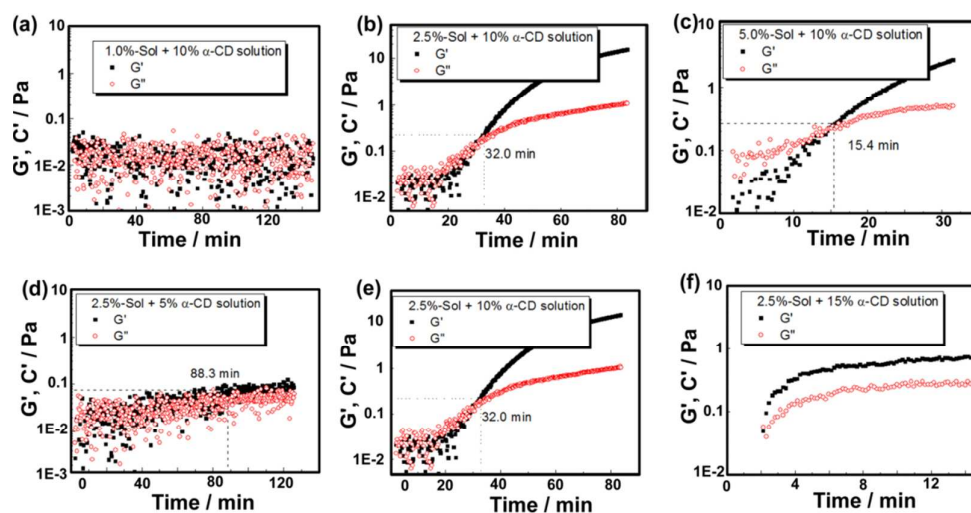
Figure 7. (a)-(c) The gelation kinetics of different colloidal QD/PEG-PCL-SH samples mixed with 10% α-CD solution. (d)-(f) The gelation kinetics of 2.5%-Sol samples mixed with different concentration of α-CD solution.
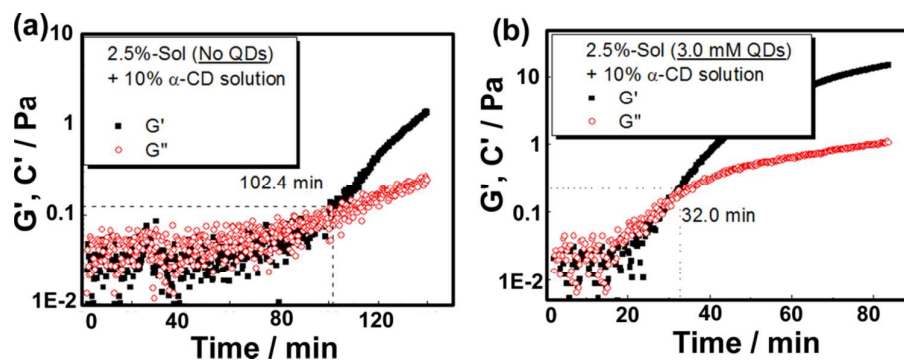

Figure 8. The gelation kinetics of (a) native hydrogel and (b) hybrid hydrogel incorporated with QDs.

RSC Advances Accepted Manuscript

Reference

1 A. H. Faraji and P. Wipf, *Bioorganic Med. Chem.*, 2009, **17**, 2950–2962.

2 a N. Shipway, E. Katz and I. Willner, *Angew. Chemie*, 2000, **39**, 19–52.

3 M. Holzinger, A. Le Goff and S. Cosnier, *Front. Chem.*, 2014, **2**, 1–10.

4 Z. Cao and B. Wei, *Energy Environ. Sci.*, 2013, **6**, 3183–3201.

5 T. Ando, *NPG Asia. Mater.*, 2009, **1**, 17–21.

6 C. M. Lieber, *MRS Bull.*, 2011, 36, 1052-1063.

7 X. Xie, A. M. Xu, M. R. Angle, N. Tayebi, P. Verma and N. a. Melosh, *Nano Lett.*, 2013, **13**, 6002–6008.

8 X. Xie, A. M. Xu, S. Leal-Ortiz, Y. Cao, C. C. Garner and N. a Melosh, *ACS Nano*, 2013, **7**, 4351–4358.

9 F. Tang, L. Li and D. Chen, *Adv. Mater.*, 2012, **24**, 1504–1534.

10 A. M. Xu, A. Aalipour, S. Leal-Ortiz, A. H. Mekhdjian, X. Xie, A. R. Dunn, C. C. Garner and N. a Melosh, *Nat. Commun.*, 2014, **5**, 3613.

11 X. Xie and N. a. Melosh, *J. Mater. Chem. B*, 2015.

12 S. Chaudhary, M. Ozkan and W. C. W. Chan, *Appl. Phys. Lett.*, 2004, **84**, 2925–2927.

13 T. Yoshie, a Scherer, J. Hendrickson, G. Khitrova, H. M. Gibbs, G. Rupper, C. Ell, O. B. Shchekin and D. G. Deppe, *Nature*, 2004, **432**, 200–203.

14 C.-A. J. Lin, T. Liedl, R. a. Sperling, M. T. Fernandez-Arguelles, J. M. Costa-Fernandez, R. Pereiro, A. Sanz-Medel, W. H. Chang and W. J. Parak, *J. Mater. Chem.*, 2007, **17**, 1343.

15 X. Gao, Y. Cui, R. M. Levenson, L. W. K. Chung and S. Nie, *Nat. Biotechnol.*, 2004, **22**, 969–976.

16 X.-L. Su and Y. Li, *Anal. Chem.*, 2004, **76**, 4806–4810.

17 R. E. Bailey, A. M. Smith and S. Nie, *Phys. E Low-Dimensional Syst. Nanostructures*, 2004, **25**, 1–12.

18 A. J. Sutherland, *Curr. Opin. Solid State Mater. Sci.*, 2002, **6**, 365–370.

19 D. Wang, Y. Cao, X. Zhang, Z. Liu, X. Qian, X. Ai, F. Liu, D. Wang, Y. Bai, T. Li and X. Tang, *Chem. Mater.*, 1999, **2**, 392–398.

20 H. Yusuf, W. G. Kim, D. H. Lee, Y. Guo and M. G. Moffitt, *Langmuir*, 2007, **23**, 868–878.

21 M. Han, X. Gao, J. Z. Su and S. Nie, *Nat. Biotechnol.*, 2001, **19**, 631–635.

22 I. L. Medintz, H. T. Uyeda, E. R. Goldman and H. Mattoussi, *Nat. Mater.*, 2005, **4**, 435–446.

23 Y. Zhang and T. H. Wang, *Theranostics*, 2012, **2**, 631–654.

24 H. Sun, L. Wu, W. Wei and X. Qu, *Mater. Today*, 2013, **16**, 433–442.

25 H. Zhao, E. P. Douglas, B. S. Harrison and K. S. Schanze, *Langmuir*, 2001, **17**, 8428–8433.

26 R. Xie, U. Kolb, J. Li, T. Basché and A. Mews, *J. Am. Chem. Soc.*, 2005, **127**, 7480–7488.

27 M. J. Murcia, D. E. Minner, G. M. Mustata, K. Ritchie and C. a. Naumann, *J. Am. Chem. Soc.*, 2008, **130**, 15054–15062.

28 J. Y. Lee, D. Heon Nam, M. H. Oh, Y. Kim, H. S. Choi, D. Y. Jeon, C. B. Park and Y. S. Nam, *Nanotechnology*, 2014, **25**, 175702.

29 A. S. Hoffman, *Adv. Drug Deliv. Rev.*, 2012, **64**, 18–23.

30 T. R. Hoare and D. S. Kohane, *Polymer*, 2008, **49**, 1993–2007.

31 G. D. Nicodemus and S. J. Bryant, *Tissue Eng. Part B. Rev.*, 2008, **14**, 149–165.

32 A. Mateescu, Y. Wang, J. Dostalek and U. Jonas, *Membranes*, 2012, **2**, 49–69.

33 B. Vilozny, A. Schiller, R. a. Wessling and B. Singaram, *J. Mater. Chem.*, 2011, **21**, 7589.

34 W. Wu, T. Zhou, J. Shen and S. Zhou, *Chem. Commun.*, 2009, 4390–4392.

35 S. Bhuniya and B. H. Kim, *Chem. Commun.*, 2006, 1842–1844.

36 J. Zhou and H. Li, *ACS Appl. Mater. Interfaces*, 2012, **4**, 721–724.

37 R. Nishiyabu, H. Kobayashi and Y. Kubo, *RSC Adv.*, 2012, **2**, 6555.

38 H. Maruyama, T. Masuda and F. Arai, *J. Robot. Mechatronics*, 2013, **25**, 596–602.

39 W. Zhan, G. H. Seong and R. M. Crooks, *Anal. Chem.*, 2002, **74**, 4647–4652.

40 C. Chang, J. Peng, L. Zhang and D.-W. Pang, *J. Mater. Chem.*, 2009, **19**, 7771.

41 K. Gatta´s-Asfura, Y. Zheng, M. Micic, M. J. Snedaker, X. Ji, G. Sui, J. Orbulescu, F. M. Andreopoulos, S. M. Pham, C. Wang and R. M. Leblanc, *J. Phys. Chem. B*, 2003, **107**, 10464–10469.

42 X. Cao, C. M. Li, H. Bao, Q. Bao and H. Dong, *Chem. Mater.*, 2007, **19**, 3773–3779.

43 Y. Tang, C. L. Heaysman, S. Willis and A. L. Lewis, *Expert Opin. Drug Deliv.*, 2011, **8**, 1141–1159.

44 J. Li and X. J. Loh, *Adv. Drug Deliv. Rev.*, 2008, **60**, 1000–1017.

45 S.-P. Zhao, L.-M. Zhang and D. Ma, *J. Phys. Chem. B*, 2006, **110**, 12225–12229.

46 D. Ma, L. M. Zhang, X. Xie, T. Liu and M. Q. Xie, *J. Colloid Interface Sci.*, 2011, **359**, 399–406.

47 H. Yu, Z. G. Feng, A. Y. Zhang, D. Hou and L. G. Sun, *Polymer*, 2006, **47**, 6066–6071.

48 X. X. andLi-M. Z. Dong Ma, *J. Polym. Sci. Part B Polym. Phys.*, 2009, **47**, 740–749.

49 H. Zhang, L. Wang, H. Xiong, L. Hu, B. Yang and W. Li, *Adv. Mater.*, 2003, **15**, 1712–1715.

50 H. Zhang and B. Yang, *Thin Solid Films*, 2002, **418**, 169–174.

51 C. X. F. Lam, D. W. Hutmacher, J.-T. Schantz, M. A. Woodruff and S. H. Teoh, *J. Biomed. Mater. Res. A*, 2009, **90**, 906–919.

52 A. Harada, J. Li and M. Kamachi, *Macromolecules*, 1993, **26**, 5698–5703.

53 K. M. Huh, T. Ooya, W. K. Lee, S. Sasaki, I. C. Kwon, S. Y. Jeong and N. Yui, *Macromolecules*, 2001, **34**, 8657–8662.

54 J. C. Ro and I. J. Chung, *J. Non. Cryst. Solids*, 1990, **126**, 259–266.

55 J. Li, X. Li, X. Ni, X. Wang, H. Li and K. W. Leong, *Biomaterials*, 2006, **27**, 4132–4140.

56 G. Carrot, S. M. Scholz, C. J. G. Plummer, J. G. Hilborn and J. L. Hedrick, *Chem. Mater.*, 1999, **11**, 3571–3577.

57 F. Winter, H. Henning, Chambon, *J. Rheol.*, 1986, **30**, 367.

58 D. Ma and L. M. Zhang, *J. Phys. Chem. B*, 2008, **112**, 6315–6321.